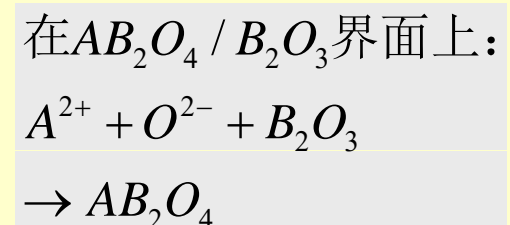# 尖晶石生成反应实例(可行性分析):
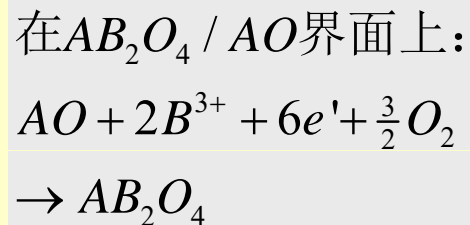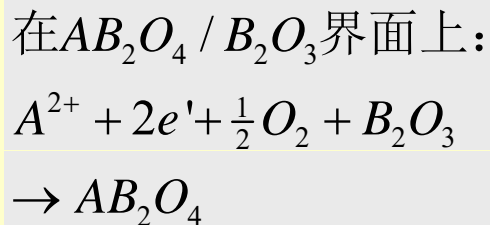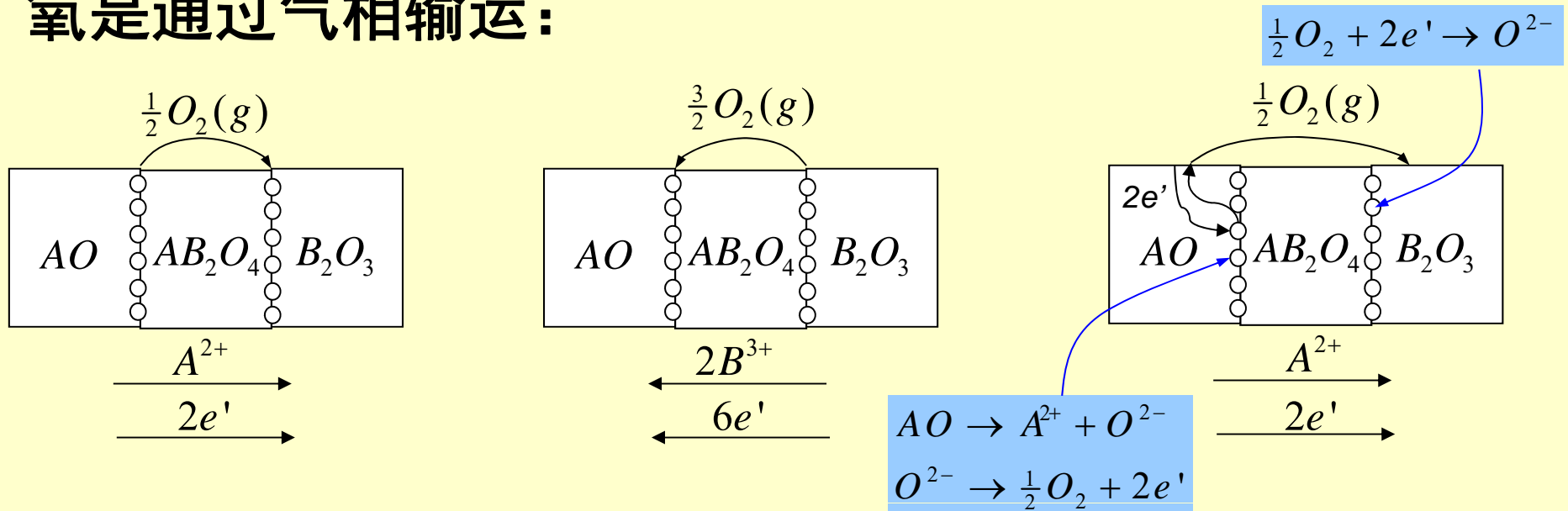
反应物及产物的结构:

- MgO 为面心立方结构（Mg^{2+}占据氧离子密堆积的八面体间隙），熔点：2852℃

- Al_2O_3为刚玉型结构（氧离子以畸变的六方密堆积排列），熔点： 2050℃

- $MgAl_2O_4$的结构与MgO的近似（氧离子面心立方密堆积， 但Mg^{2+}占四面体间隙，Al^{3+} 占八面体间隙），熔点： 2100℃

- 因此，由MgO 和Al_2O_3反应生成$MgAl_2O_4$的初期（成核反应），需要很高的活化能（共价键键能很高），同时需要较大距离的离子迁移和重排。

AO(s) + B₂O₃(s)→AB₂O₄(s) 的 反 应 机 理

对于由氧化物（**AO和B₂O₃**）合成尖晶石（**AB₂O₄**）的反应，合理的反应机理假设有4种，其中三种机理认为氧是通过气相输运：

$$\tfrac{1}{2}O_2 + 2e' \rightarrow O^{2-}$$

$$\tfrac{1}{2}O_2(g)$$

$$\tfrac{3}{2}O_2(g)$$

$$\tfrac{1}{2}O_2(g)$$

AO	AB₂O₄	B₂O₃

$$A^{2+}$$
$$2e'$$

AO	AB₂O₄	B₂O₃

$$2B^{3+}$$
$$6e'$$

$$AO \rightarrow A^{2+} + O^{2-}$$
$$O^{2-} \rightarrow \tfrac{1}{2}O_2 + 2e'$$

$$2e'$$
AO	AB₂O₄	B₂O₃

$$A^{2+}$$
$$2e'$$

在 AB_2O_4 / B_2O_3 界面上:
$A^{2+} + 2e' + \tfrac{1}{2}O_2 + B_2O_3$
$\rightarrow AB_2O_4$

在 AB_2O_4 / AO 界面上:
$AO + 2B^{3+} + 6e' + \tfrac{3}{2}O_2$
$\rightarrow AB_2O_4$

在 AB_2O_4 / B_2O_3 界面上:
$A^{2+} + O^{2-} + B_2O_3$
$\rightarrow AB_2O_4$

AO(s) + B$_2$O$_3$(s)→AB$_2$O$_4$(s) 的反应机理

这三种机理都是假定氧通过气相输运，一种金属阳离子和对应电荷数的电子通过产物的扩散，这在**AO**与**B$_2$O$_3$**呈点接触或线（晶棱）接触时，或许是可能的，但反应速度会相当慢（反应接触面很小）
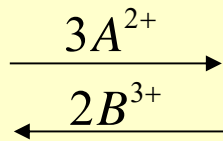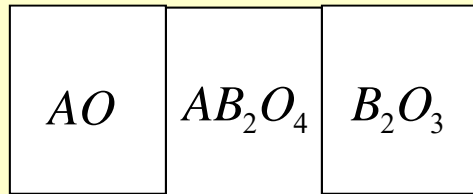
氧通过气相输运的假定，对于形成连续致密产物膜（层）的反应系统，不能成立；另外，机理还假定反应产物是电子导电的，这在某些实际系统中或许可以满足。
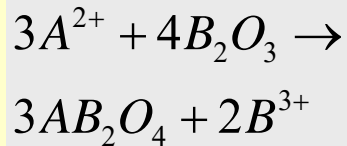
结论：一旦产物形成连续的致密膜（层），氧通过气相输运的假定将不再成立。

AO(s) + B₂O₃(s)→AB₂O₄(s) 的反应机理
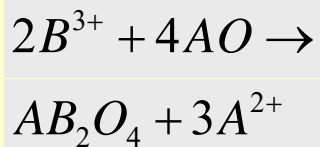
另一种机理认为，反应物以离子扩散形式通过产物层：
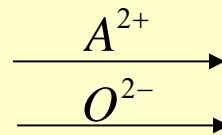
$$D_{A^{2+}} \sim D_{B^{3+}}$$

AO	AB_2O_4	B_2O_3

$$\xrightarrow{\quad 3A^{2+} \quad}$$
$$\xleftarrow{\quad 2B^{3+} \quad}$$

在 AB_2O_4 / B_2O_3 界面上：

$3A^{2+} + 4B_2O_3 \rightarrow$

$3AB_2O_4 + 2B^{3+}$

在 AB_2O_4 / AO 界面上：

$2B^{3+} + 4AO \rightarrow$

$AB_2O_4 + 3A^{2+}$

$$D_{A^{2+}} >> D_{B^{3+}}$$

AO	AB_2O_4	B_2O_3

$$\xrightarrow{\quad A^{2+} \quad}$$
$$\xrightarrow{\quad O^{2-} \quad}$$

在 AB_2O_4 / B_2O_3 界面上：

$A^{2+} + O^{2-} + B_2O_3$

$\rightarrow AB_2O_4$

$$D_{A^{2+}} << D_{B^{3+}}$$

AO	AB_2O_4	B_2O_3

$$\xleftarrow{\quad 2B^{3+} \quad}$$
$$\xleftarrow{\quad 3O^{2-} \quad}$$

在 AB_2O_4 / AO 界面上：

$AO + 2B^{3+} + 3O^{2-}$
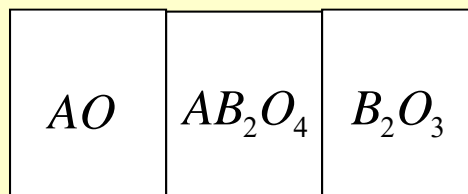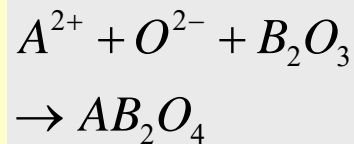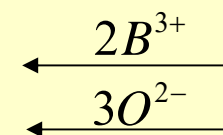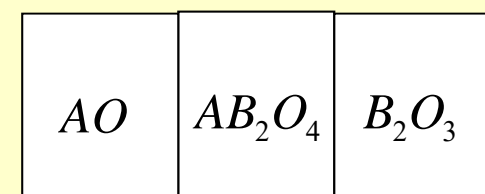
$\rightarrow AB_2O_4$
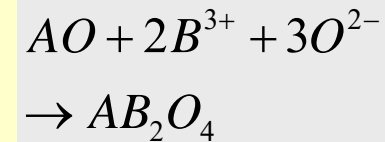
Wagner 通过对尖晶石生成反应的研究后认为，反应过程仅涉及**阳离子的对扩散**，不涉及氧离子扩散。

Diffusion coefficients

1. K^+ in β-Al_2O_3
2. O in $Ca_{0.14}Zr_{0.86}O_{1.86}$
3. Co in $Co_{1-\delta}O$ (air)
4. O in Y_2O_3
5. Cr in Cr_2O_3
6. O in $Co_{1-\delta}O$ (air)
7. N in UN
8. Co in $Co_{1-\delta}O$ ($P_{O2} = 10^{-14}$ Bar)
9. Al in α-Al_2O_3
10. Na in NaCl
11. O in $UO_{2.00}$
12. O in α-Al_2O_3 (polycrystalline)
13. O in α-Al_2O_3 (single crystalline)
14. C in graphite
15. O in Cr_2O_3
16. U in UO_2
17. O in SiO_2 (glass)
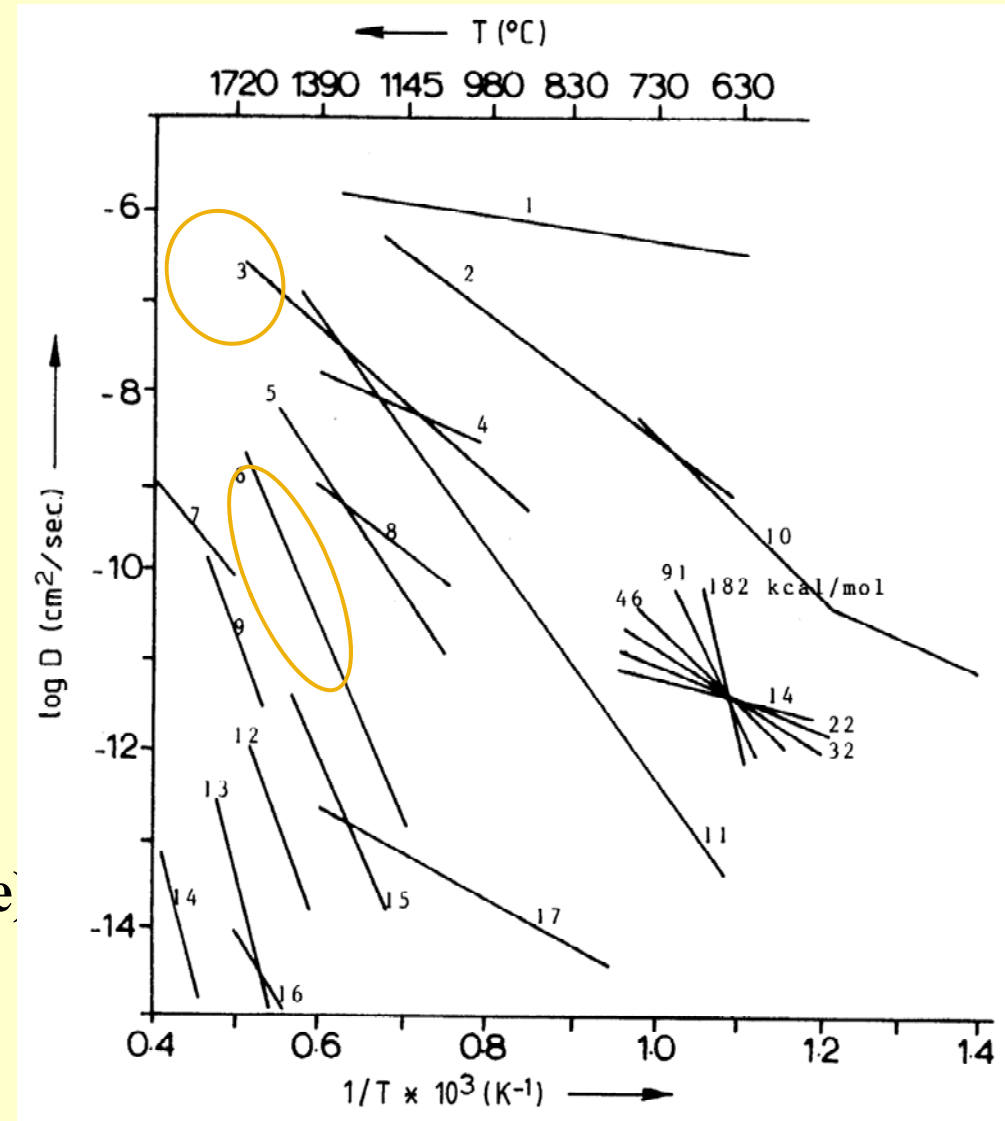
r_{Mg2+} = 72 pm r_{Al3+} = 53.5 pm r_{O2-} = 140 pm

AO(s) + B₂O₃(s)→AB₂O₄(s) 的反应机理

尖晶石的生成反应是一种多相反应，反应的阻力来自离子通过产物层和相界面，当产物层厚度足够厚时（例如：1200°C时，＞1 μm），界面层的阻力相对小到可以忽略不计，反应相界面达到局域的热力学平衡，这时，反应速率完全受物质扩散通过产物层的控制。实验测量结果显示，这时的反应速率遵守"抛物线增长定律"，即

$$\Delta x^2 \propto t \quad \text{或} \quad \Delta x^2 = 2kt$$

尖晶石生成反应速率方程推导

$$\Delta x^2 \propto t \quad \text{或} \quad \Delta x^2 = 2kt$$
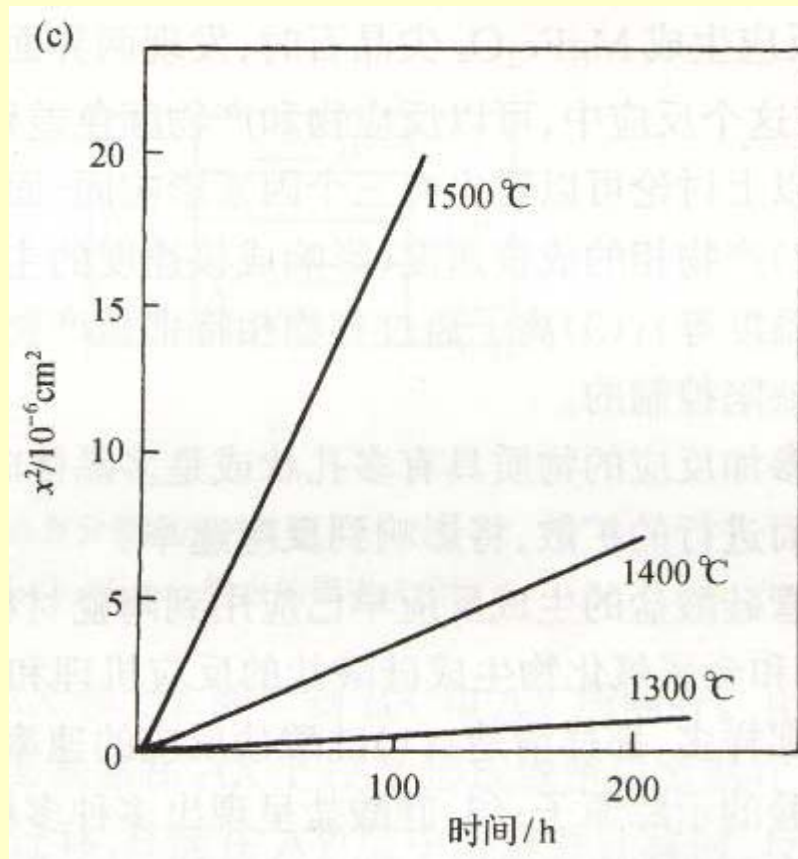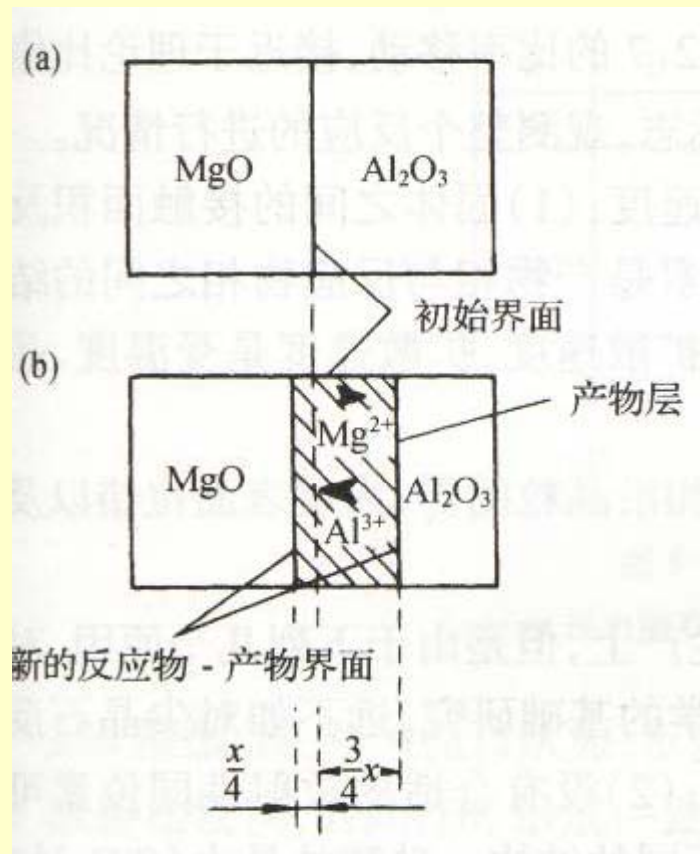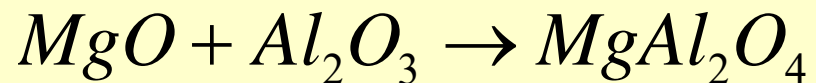
产物层厚度的增加速率正比于离子的扩散流，即

$$\frac{d\Delta x}{dt} = -\frac{dm}{\rho dt} = D\frac{dc}{\rho dx} = D\frac{\Delta c}{\rho \Delta x} (d\Delta x \text{和} dm \text{符号相反，稳态扩散）}$$

上式积分得：

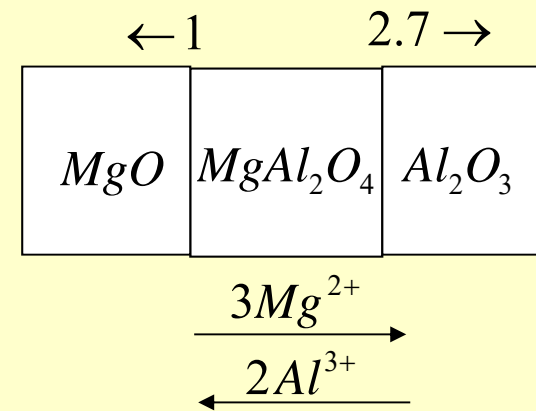$$(\Delta x)^2 = 2(\Delta cD / \rho)t \quad \text{或} \quad \Delta x^2 = 2kt \quad (k = \Delta cD / \rho)$$

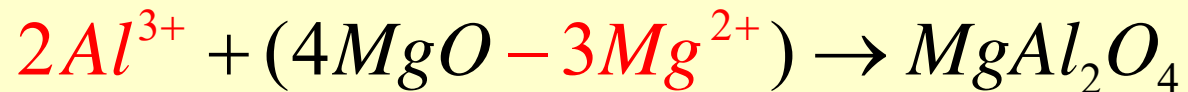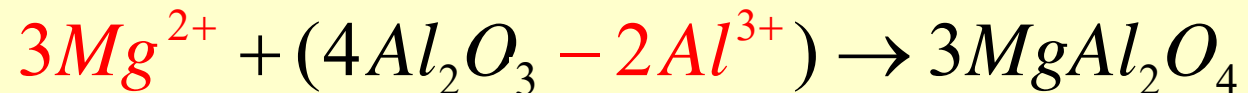稳态扩散：在扩散系统中，任一体积元在任一时刻，流入的物质量与流出的物质量相等，即任一点的浓度不随时间变化。

尖晶石生成反应实例：

$$MgO + Al_2O_3 \rightarrow MgAl_2O_4$$

1. **MgO 和 Al_2O_3 反应生成 $MgAl_2O_4$ 的初期，成核反应，困难！**

2. **$MgAl_2O_4$ 厚度增加，涉及 Mg^{2+} 和 Al^{3+} 离子通过产物层的互扩散迁移和界面上的产物生成反应。**

$\leftarrow 1 \qquad 2.7 \rightarrow$

| MgO | $MgAl_2O_4$ | Al_2O_3 |

$\xrightarrow{3Mg^{2+}}$
$\xleftarrow{2Al^{3+}}$

3. **在 MgO / $MgAl_2O_4$ 界面上：**

$$2Al^{3+} + (4MgO - 3Mg^{2+}) \rightarrow MgAl_2O_4$$

在 $MgAl_2O_4$ / Al_2O_3 界面上：

$$3Mg^{2+} + (4Al_2O_3 - 2Al^{3+}) \rightarrow 3MgAl_2O_4$$

总反应： $4MgO + 4Al_2O_4 \rightarrow 4MgAl_2O_4$ (左、右量，**1:3** 关系）

Kirkendall ratio

MgO-Al$_2$O$_3$ phase diagram
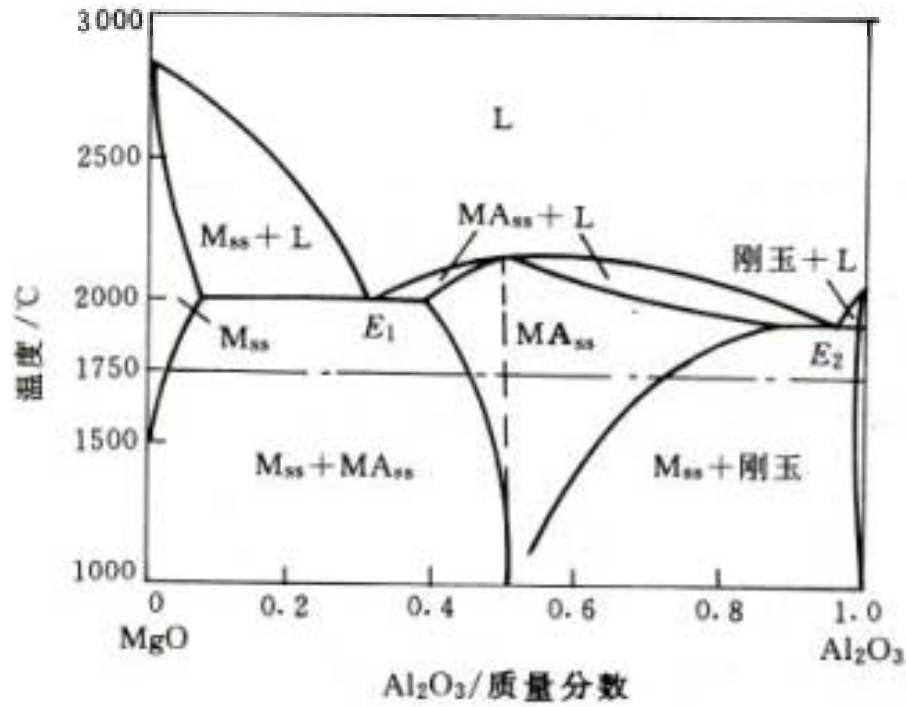
摩尔分数

MgO-Al$_2$O$_3$ 系相图

L-液体；SS-固溶体
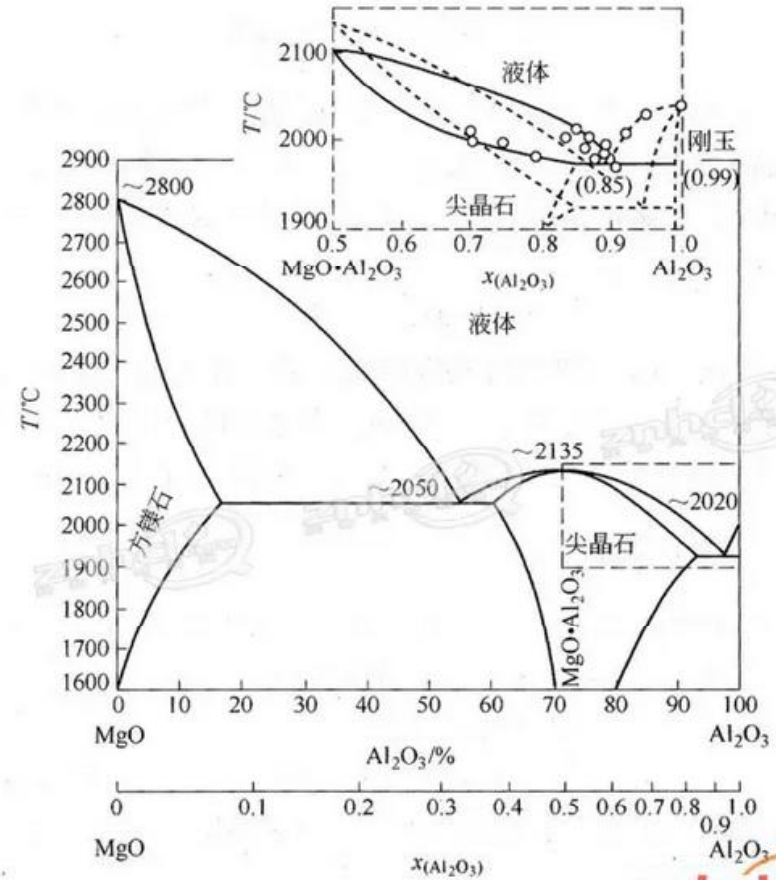
MgO-Al$_2$O$_3$ 相图

FACTORS INFLUENCING CATION DIFFUSION RATES IN SOLID STATE REACTIONS: $MgO+Al_2O_3$

- Lattice of oxide anions, mobile Mg^{2+} and Al^{3+} cations

- Factors influencing cation diffusion rates

⇨ Charge, mass and temperature

⇨ Interstitial Frenkel versus substitutional Schottky diffusion

- Depends on number and types of defects in reactant and product phases

⇨ Point, line, planar defects, grain boundaries

⇨ Enhanced ionic diffusion with defects and grain boundaries

KIRKENDALL EFFECT

OTHER SOLID STATE REACTIONS

- **MgO + Fe$_2$O$_3$ → MgFe$_2$O$_4$**
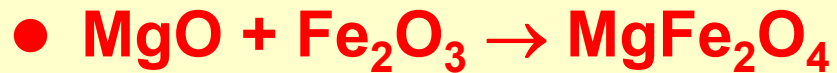
⇨ **Different color interfaces**

⇨ **Easily monitored rates**

- **Other examples - calculate the Kirkendall ratio:**

⇨ **SrO + TiO$_2$ → SrTiO$_3$ Perovskite, AMO$_3$ (type ReO$_3$)**

⇨ **2KF + NiF$_2$ → K$_2$NiF$_4$**
Corner Sharing Oh NiF$_6^{2-}$ Sheets, Inter-sheet K$^+$

⇨ **2SiO$_2$ + Li$_2$O → Li$_2$Si$_2$O$_5$**

7.5.1.2 硅酸盐合成反应

"简单"反应：$2CaO(s) + SiO_2(s) \rightarrow Ca_2SiO_4(s)$

几种可能的扩散反应机理

Diffusion Mechanism   **Diffusion Reaction**

$+ SiO_2$

$2Ca^{2+} + 2O^= \rightarrow Ca_2SiO_4$ √

$2Ca^{2+} + 2SiO_2 \rightarrow Ca_2SiO_4 + Si^{4+}$
$Si^{4+} + 4CaO \rightarrow Ca_2SiO_4 + 2Ca^{2+}$

$2O^= \rightarrow O_2\uparrow + 4e^-$
$2CaO + O_2\uparrow + 4e^- \rightarrow Ca_2SiO_4$
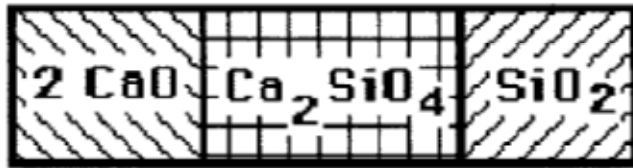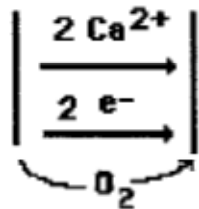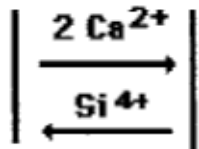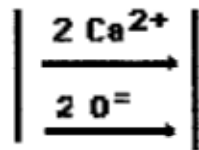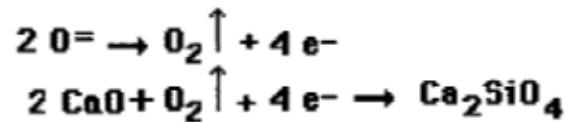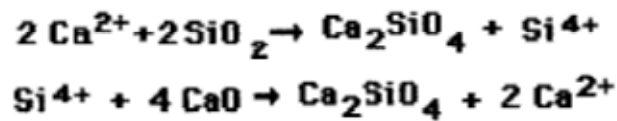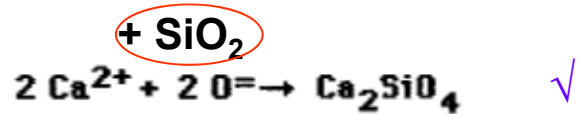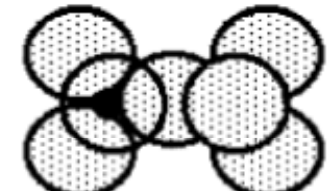
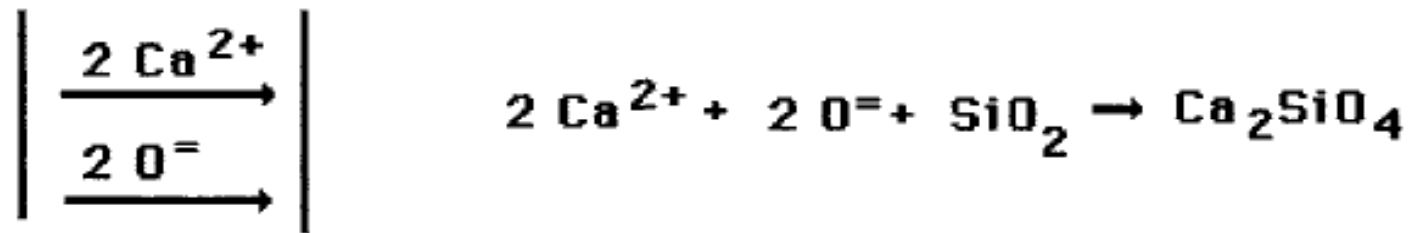Disilicate Tetrahedra   Position of Si^{4+} Atoms in Tetrahedra

$$D_{Ca^{2+}} \cong D_{O^{2-}} >> D_{Si^{4+}}$$

所以，主导扩散反应机理：

$$2Ca^{2+} + 2O^{=} + SiO_2 \rightarrow Ca_2SiO_4$$

上述反应基于一个假设：相界面层在生成后不再发生其它变化。实际上，变化是可能的。

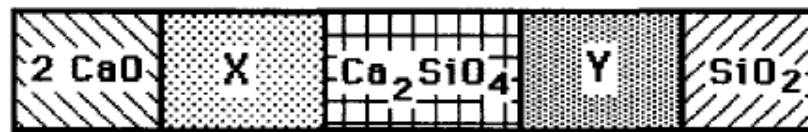$$Ca^{2+} + O^{=} + Ca_2SiO_4 \rightarrow Ca_3SiO_5$$

$$Si^{4+} + 2O^{=} + 3Ca_2SiO_4 \rightarrow 2Ca_3Si_2O_7$$

$$3Ca^{2+} + 3O^{2-} + 2SiO_2 \rightarrow Ca_3Si_2O_7$$
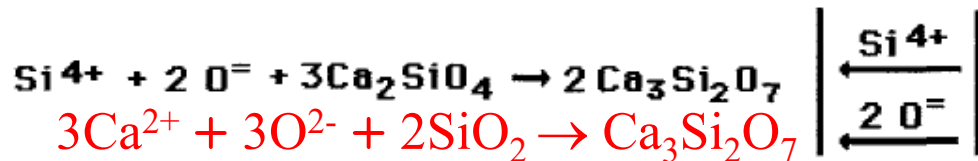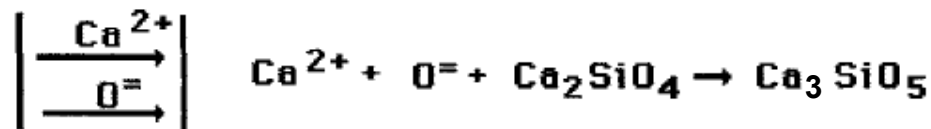
注："Si^{4+}"的扩散实际上代表某种"SiO$_n$"$^{\delta+}$的扩散。

"简单"反应：$2CaO(s) + SiO_2(s) \rightarrow Ca_2SiO_4(s)$
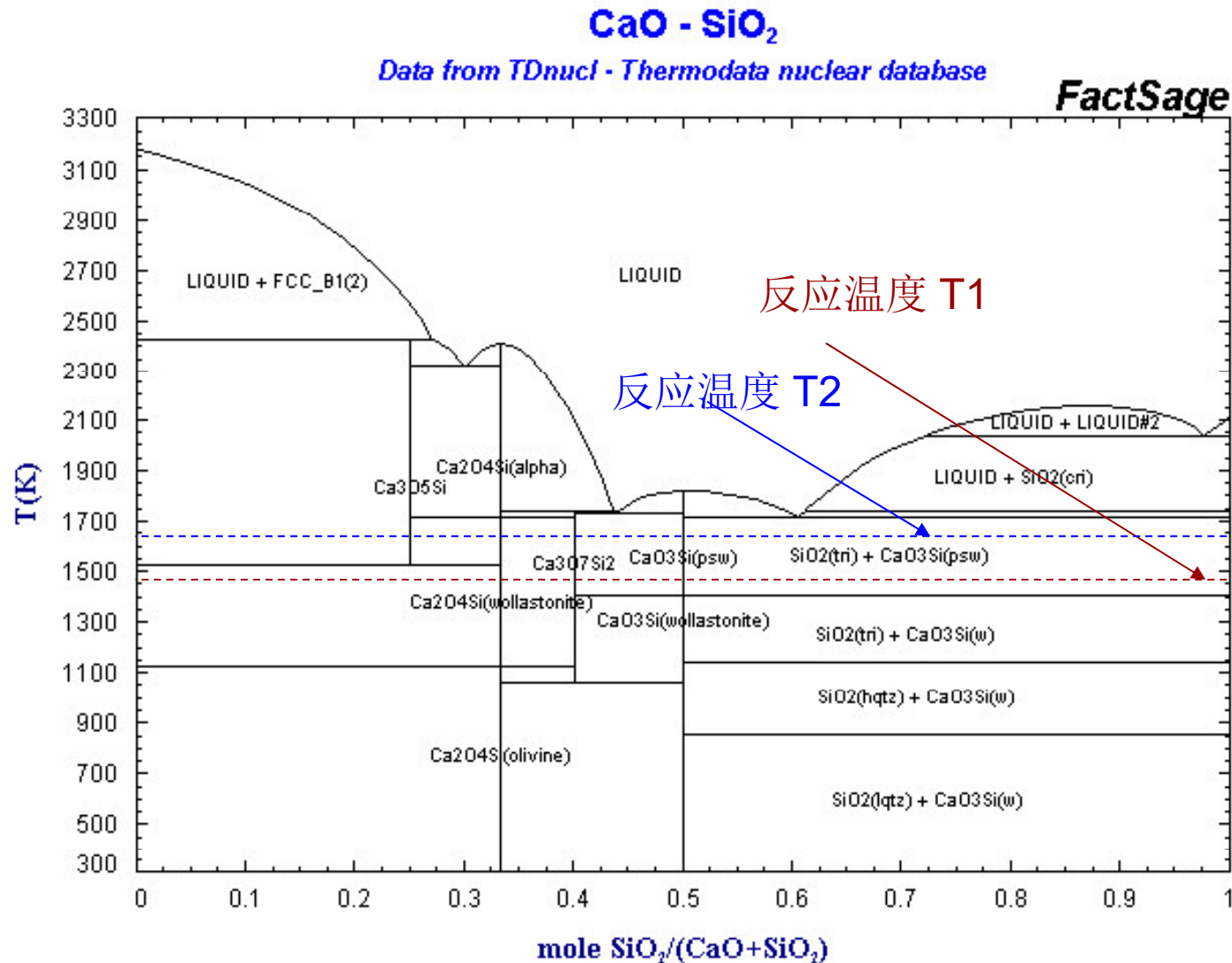
在实际使用的反应温度**T1**下**Ca₃SiO₅**不存在，但**Ca₃Si₂O₇**存在。

"简单"反应：$2CaO(s) + SiO_2(s) \rightarrow Ca_2SiO_4(s)$

所以，在右侧界面附近还有一层**Ca₃Si₂O₇**的生成，因此在**Ca₃Si₂O₇/Ca₂SiO₄**界面的反应为：

$$Ca^{2+} + O^{2-} + Ca_3Si_2O_7 \rightarrow 2Ca_2SiO_4$$
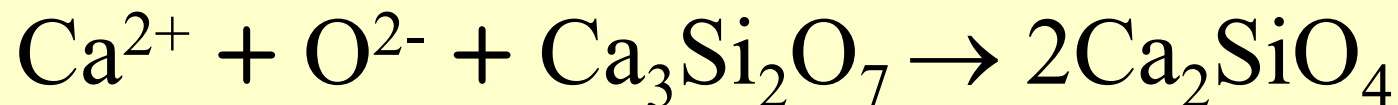
Ca²⁺ 和 **O²⁻** 穿过**Ca₃Si₂O₇**和**Ca₂SiO₄**两层到达**SiO₂**界面，可以发生反应生成偏硅酸盐：
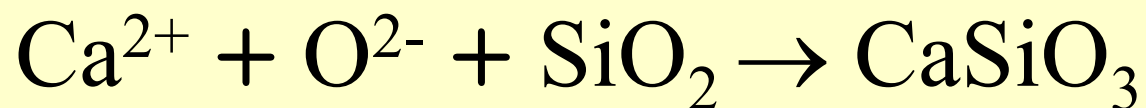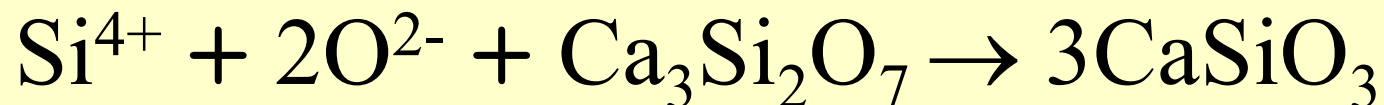
$$Ca^{2+} + O^{2-} + SiO_2 \rightarrow CaSiO_3$$

同样，在相对的方向有：

$$Si^{4+} + 2O^{2-} + Ca_3Si_2O_7 \rightarrow 3CaSiO_3$$

"简单"反应：$2CaO(s) + SiO_2(s) \rightarrow Ca_2SiO_4(s)$
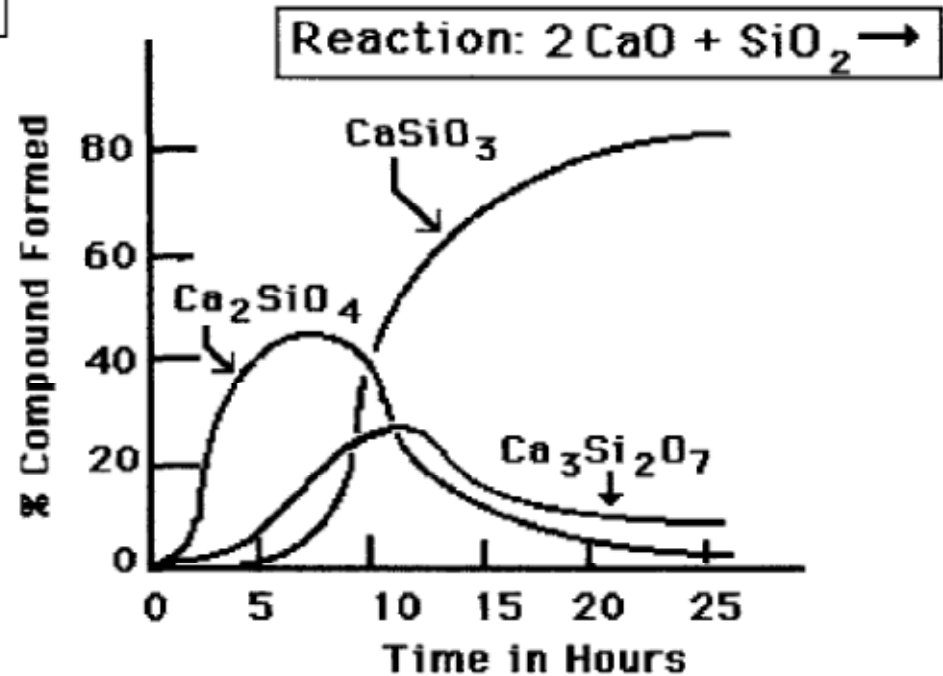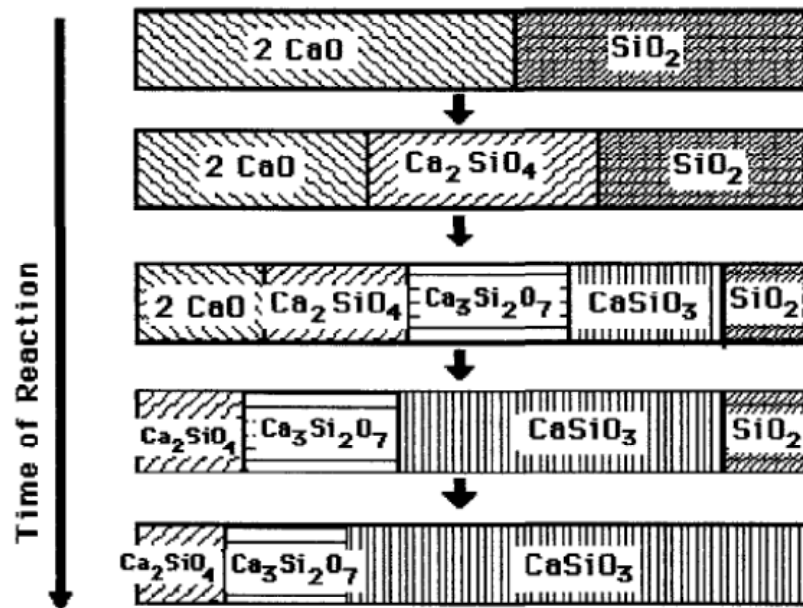
所以，**2CaO:SiO₂**通过<u>扩散控制</u>的固相反应，反应产物总是混合物（以偏硅酸盐为主，加上少量富钙的硅酸盐相。实际上，**CaO:SiO₂**原料组成得到相似结果，只不过产物中**Ca₂SiO₄**和**Ca₃Si₂O₇**相更少。

类似反应：$1.0\ BaO + 1.0\ SiO_2$
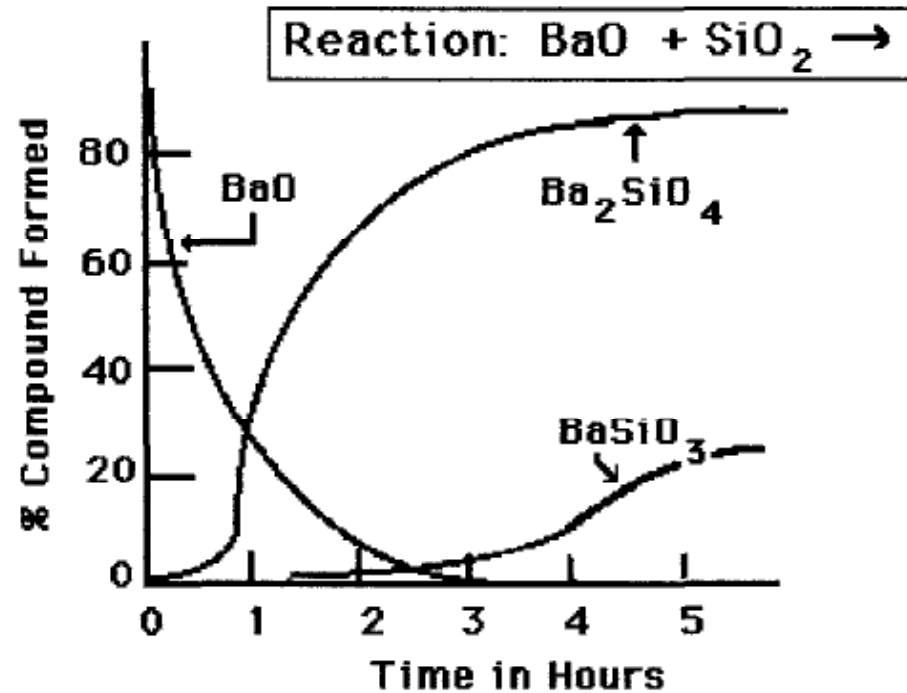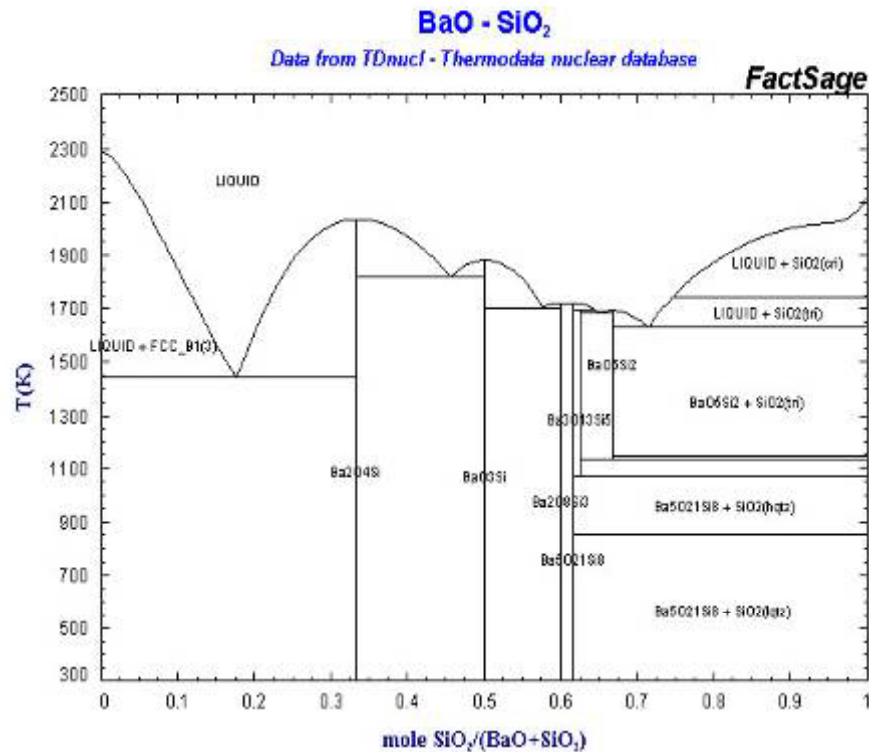
反应产物主相是**Ba₂SiO₄**！

结论：耐熔氧化物间通过扩散控制的固相反应的产物总是混合物。

如何得到纯相的产物？

1. 采用气相反应。（很难找到气态反应物）
2. 添加助熔剂。（难以找到不干扰反应的助熔剂）
3. 使用强反应活性组份。（避免扩散控制）
4. 用沉淀产物作为反应基础。

$$2\ BaCO_3 + SiO_2 \Rightarrow Ba_2SiO_4\ (100\%\ yield)$$
$$BaCO_3 + SiO_2 \Rightarrow BaSiO_3\ (100\%\ yield)$$
$$3\ BaCO_3 + SiO_2 \Rightarrow Ba_3SiO_5\ (100\%\ yield)$$

$$BaCO_3 \rightarrow BaO + CO_2$$
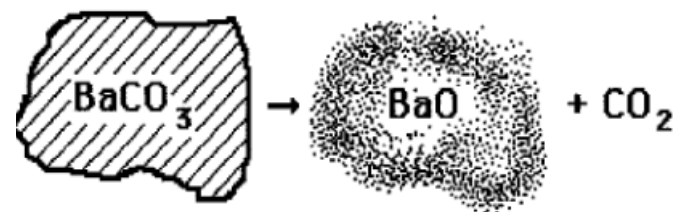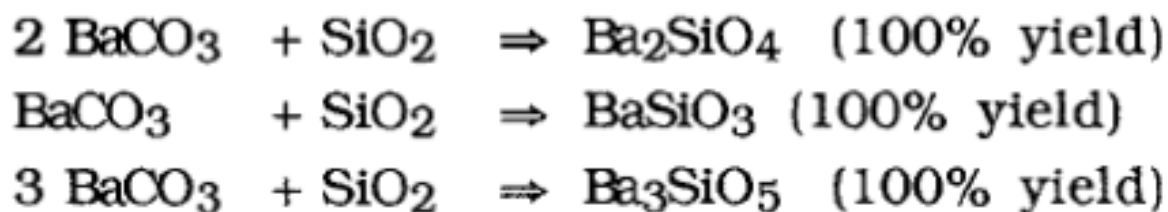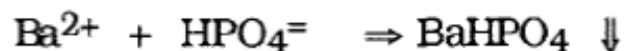
先沉淀反应 $Ba^{2+} + HPO_4^{=} \Rightarrow BaHPO_4 \Downarrow$ 再与**BaCO₃**反应得到 **100%Ba₃(PO₄)₂**产率。

$$2\ BaHPO_4 + BaCO_3 \Rightarrow Ba_3(PO_4)_2 + H_2O \Uparrow + CO_2 \Uparrow$$

反应：NiO(s) + Al$_2$O$_3$(s)→NiAl$_2$O$_4$(s)

NiO | NiAl$_2$O$_4$ | Al$_2$O$_3$

Diffusion Mechanism　　**Diffusion Reaction**

3 Ni^{2+} →
← 2 Al^{3+}

3 Ni^{2+} + 4 Al$_2$O$_3$ → 3 NiAl$_2$O$_4$ + 2 Al^{3+}

2Al^{3+}+4NiO→NiAl$_2$O$_4$ + 3Ni^{2+}

Ni^{2+} →
O$^=$ →

Ni^{2+} + O$^=$ +Al$_2$O$_3$ → NiAl$_2$O$_4$

← 2 Al^{3+}
← 3 O$^=$

2 Al^{3+} + NiO + 3 O$^=$ → NiAl$_2$O$_4$
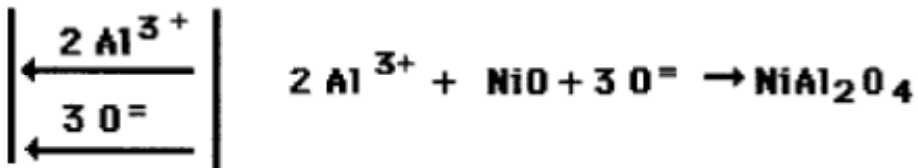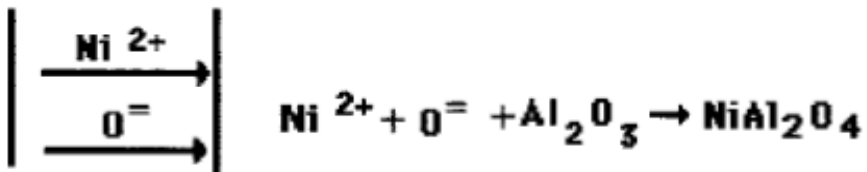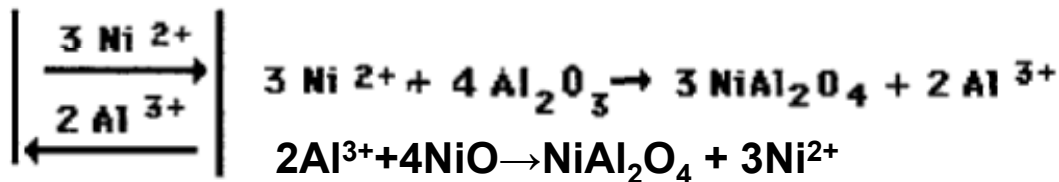
左边是可能的反应机理。

但是，如果部分Ni^{2+}氧化到Ni^{3+}，则情形会有不同--- 会有镍离子空位产生，即Ni$_{1-\delta}$Al$_2$O$_4$.

反应：$NiO(s) + Al_2O_3(s) \rightarrow NiAl_2O_4(s)$

所以，产物结构可能如下所示，有一层$Ni_{1-\delta}Al_2O_4$和$NiAlO_3$：

反应机理还包括下面两个（缺陷固相反应）：

$Ni_{1-\delta}Al_2O_4$

$$Ni^{3+} + O^= + Al_2O_3 + V_{Ni}^- \rightarrow NiV_{Ni}Al_2O_4$$

$$2Ni^{3+} + 2Al_2O_3 + 4NiO \rightarrow 2NiAlO_3 + NiAl_2O_4 + 3Ni^{2+}$$

$$Ni^{3+} + Al_2O_3 \rightarrow NiAlO_3 + Al^{3+}$$
$$Al^{3+} + 4NiO \rightarrow NiAl_2O_4 + 3Ni^{2+}$$
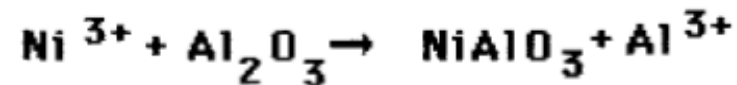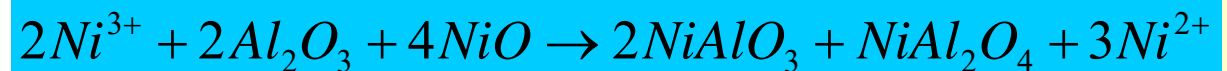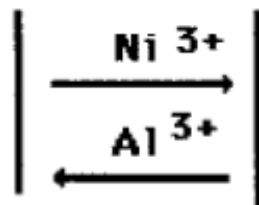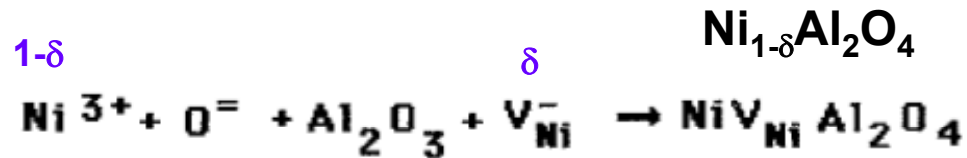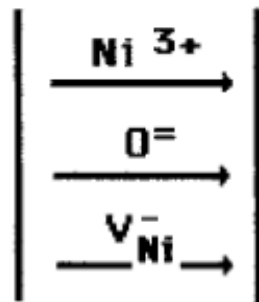
NANOCLUSTER KIRKENDALL SYNTHESIS OF HOLLOW NANOCLUSTERS
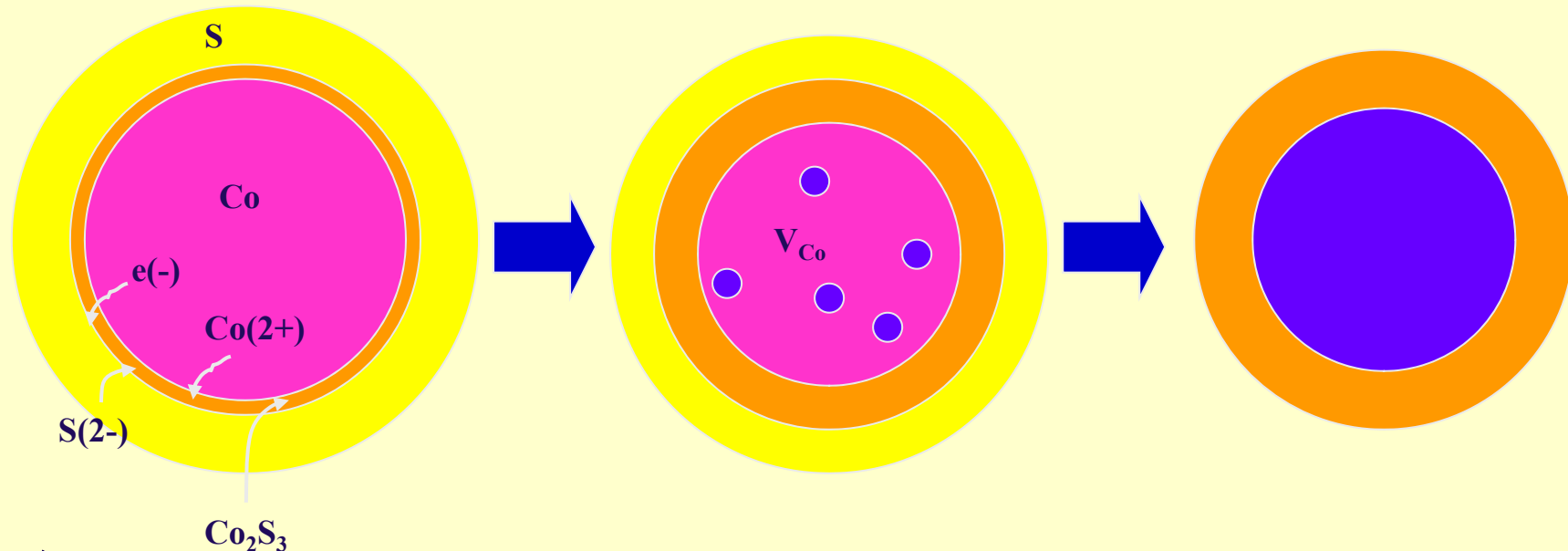
1）**Capped cobalt nanoclusters in a high temperature solvent,**
2）**sulfur injection, coating of sulfur on nanocluster, cobalt sesquisulfide product shell layer formed at interface,**
3）**counter-diffusion of $Co^{2+}/2e(-)$ and S^{2-} across thickening shell,**
4）**faster diffusion of Co^{2+} creates V_{Co} in core,**
5）**vacancies agglomerate in core, hollow core created which grows as the product shell thickens –**
6）**end result – a hollow nanosphere made of cobalt sesquisulfide Co_2S_3**

TURNING NANOSTRUCTURES INSIDE-OUT

- **The Kirkendall effect is a well-known phenomenon discovered in the 1930's.**

- **It occurs during the reaction of two solid-state materials and involves the diffusion of reactant species, like ions, across the product interface usually at different rates.**

- **In the special case when the movement of the fast-diffusing component cannot be balanced by the movement of the slow component the net mass flow is accompanied by a net flow of atomic vacancies in the opposite direction.**

- **This effect leads to Kirkendall porosity, formed through supersaturation of vacancies into hollow pores**

- **When starting with perfect building blocks such as cobalt nanocrystals a reaction meeting the Kirkendall criteria can lead to supersaturation of vacancies exclusively in the center of the nanocrystal.**

- **This provides a general route to hollow nanocrystals out of almost any given material**

- **Proof-of-concept - synthesis of a cobalt sulfide nanoshell starting from a cobalt nanocluster.**

Time evolution of a hollow cobalt sulfide nanocrystal grown from a cobalt nanocrystal via the nanoscale Kirkendall effect Y.D. Yin et al., *Science* 2004, *304*, 711
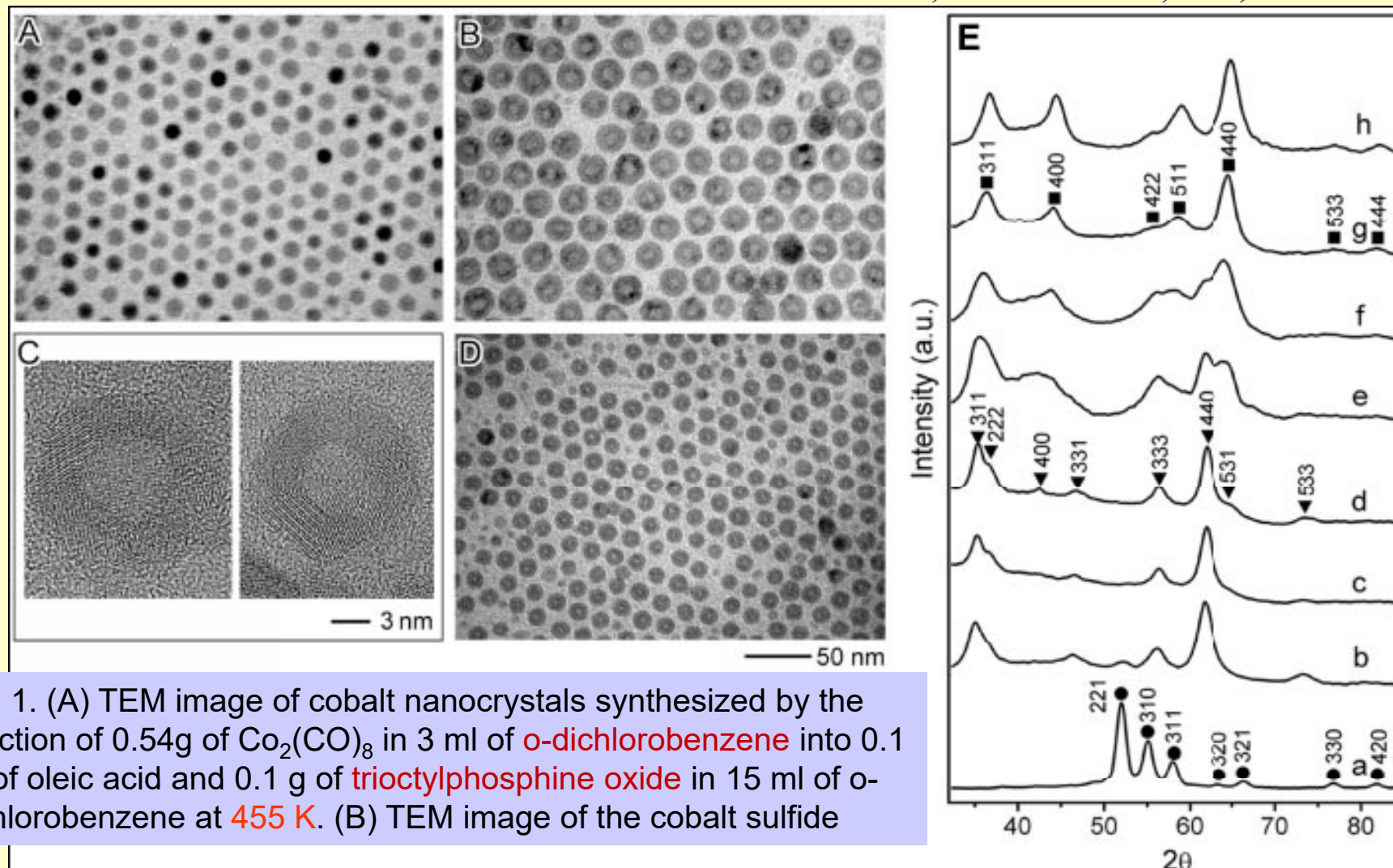

Fig. 1. (A) TEM image of cobalt nanocrystals synthesized by the injection of 0.54g of $Co_2(CO)_8$ in 3 ml of o-dichlorobenzene into 0.1 ml of oleic acid and 0.1 g of trioctylphosphine oxide in 15 ml of o-dichlorobenzene at 455 K. (B) TEM image of the cobalt sulfide phase synthesized by the injection of sulfur in o-dichlorobenzene (5 ml) into cobalt nanocrystal solution with a Co/S molar ratio of 9:12. Co_3S_4 particles were synthesized from the cobalt sample shown in (A). (C) HRTEM images of Co_3S_4 (left) and Co_9S_8 (right). (D) TEM image of the cobalt sulfide phase synthesized as in (B), but with a Co:S molar ratio of 9:8. Co_9S_8 particles started from another cobalt sample that had an average diameter of ▯ 11 nm. (E) XRD patterns of (a) cobalt nanocrystals and (b to h) cobalt sulfide synthesized with different Co/S molar ratios: (b) 9:5, (c) 9:7, (d) 9:8, (e) 9 :10, (f) 9 :11, (g) 9 :12, and (h) 9 :18. The dots, triangles, and squares represent peaks from cobalt, Co_9S_8, and Co_3S_4 phases, respectively.
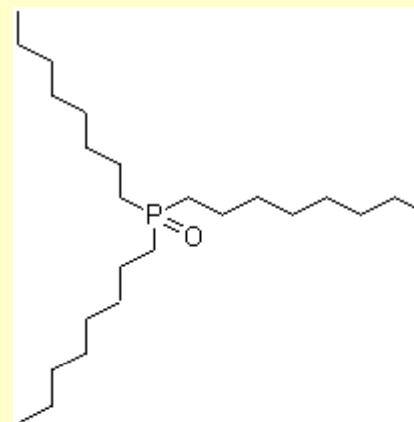
Time evolution of a hollow cobalt sulfide nanocrystal grown from a cobalt nanocrystal via the nanoscale Kirkendall effect Y.D. Yin et al., *Science* 2004, *304*, 711
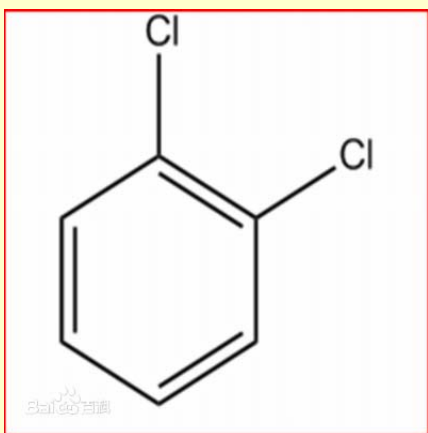
Oleic acid

o-dichlorobenzene
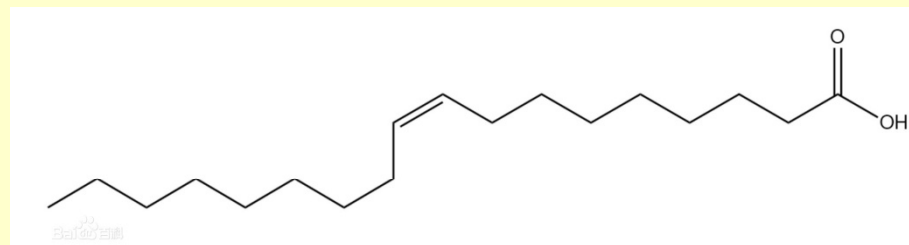
trioctylphosphine oxide

三正辛基氧膦

Time evolution of a hollow cobalt sulfide nanocrystal grown from a cobalt nanocrystal via the nanoscale Kirkendall effect Y.D. Yin et al., *Science* 2004, *304*, 711
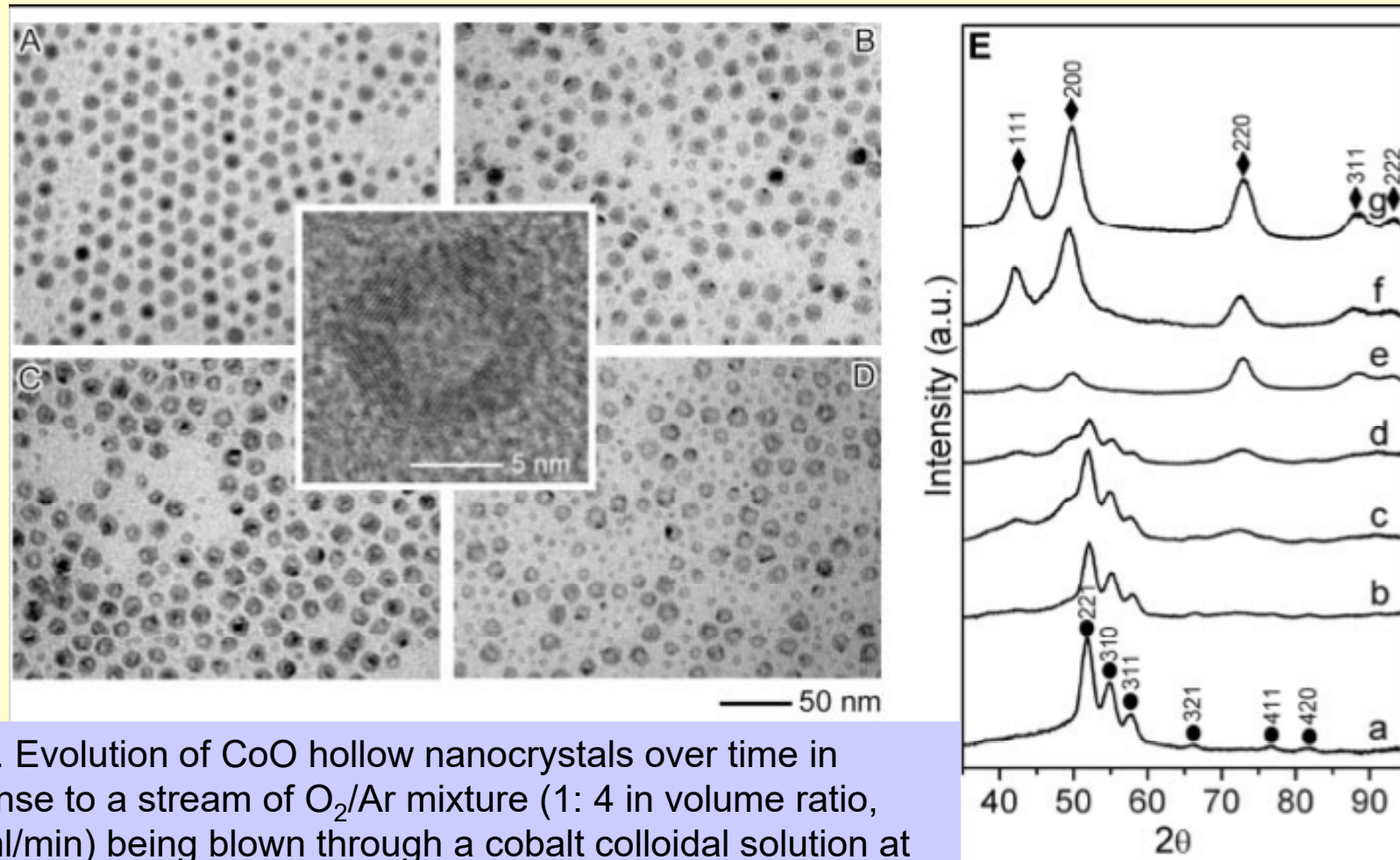

Fig. 2. Evolution of CoO hollow nanocrystals over time in response to a stream of O_2/Ar mixture (1: 4 in volume ratio, 120 ml/min) being blown through a cobalt colloidal solution at 455 K. (A to D) TEM images of the solutions after flow of O_2/Ar for (A) 0 min, (B) 30 min, (C) 80 min, and (D) 210 min. Inset: HRTEM of a CoO hollow nanocrystal. (E) XRD patterns of the sample obtained from the solution after flow of O_2/Ar for (a) 0 min, (b) 2.5 min, (c) 5.5 min, (d) 10 min, (e) 30 min, (f) 80 min, and (g) 210 min. The dots and diamonds represent peaks from cobalt and CoO phases, respectively.

Time evolution of a hollow cobalt sulfide nanocrystal grown from a cobalt nanocrystal via the nanoscale Kirkendall effect
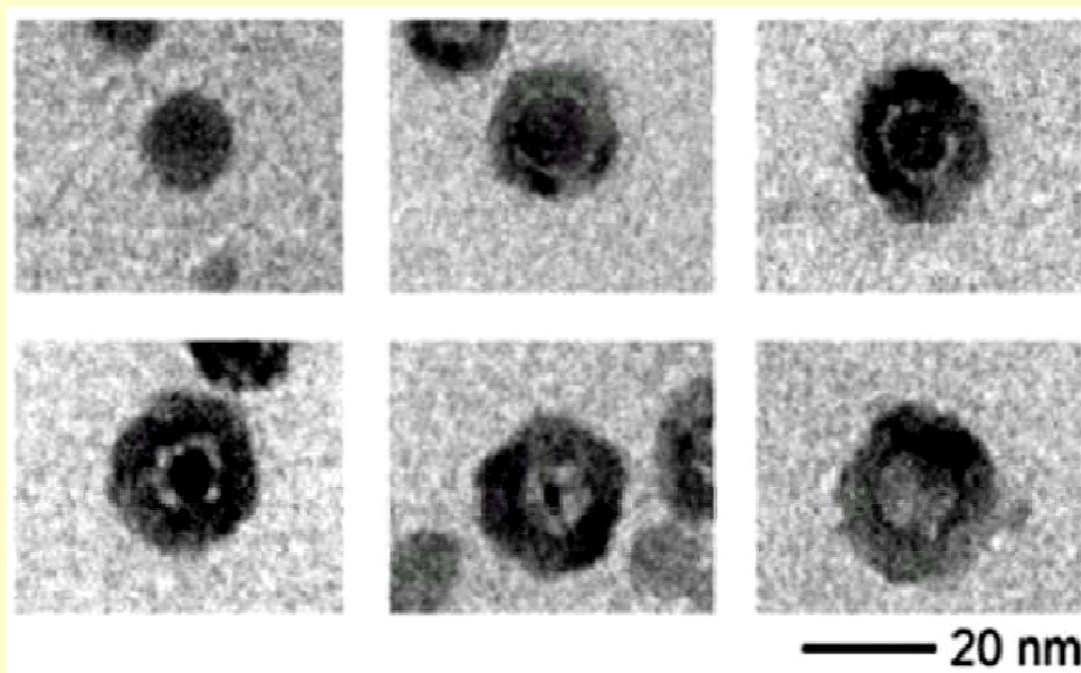## Y.D. Yin et al., *Science* 2004, *304*, 711

Fig. 3 Evolution of CoSe hollow nanocrystals with time by injection of a suspension of selenium in o-dichlorobenzene into a cobalt nanocrystal solution at 455 K, from top-left to bottom right: 0 s, 10 s, 20 s, 1min, 2 min, and 30min. The Co/Se molar ratio was 1:1.

Time evolution of a hollow cobalt sulfide nanocrystal grown from a cobalt nanocrystal via the nanoscale Kirkendall effect Y.D. Yin et al., *Science* 2004, *304*, 711
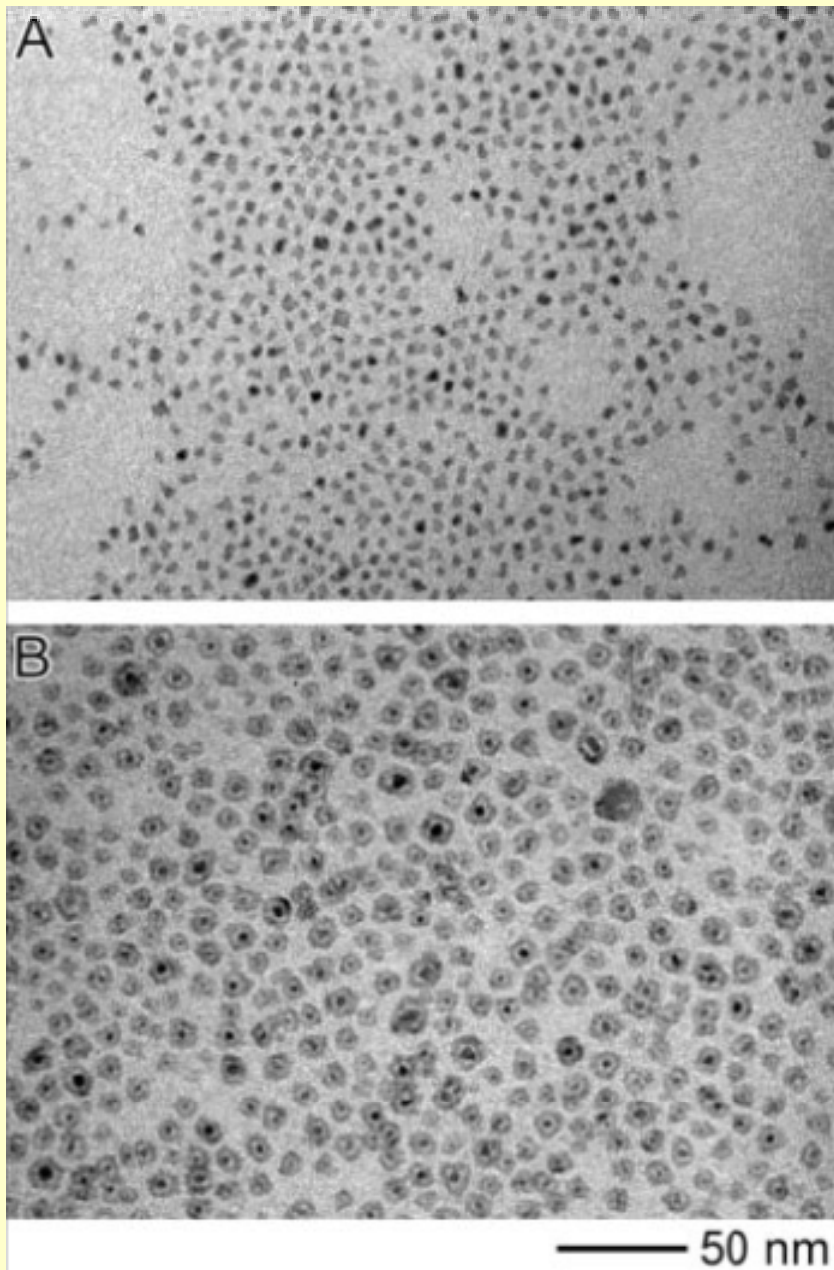

Fig. 4. (A) Platinum nanocrystals prepared by the injection of a solution of 0.15 g of platinum acetylacetonate in 5 ml of o-dichlorobenzene into a refluxing bath of 10 ml of o-dichlorobenzene that contained 0.3 g of 1,2-hexadecanediol, 0.1 ml of oleic acid, 0.1 ml of oleylamine, and 0.06 ml of trioctylphosphine. The solution was then heated for another 120 min. (B) We formed Pt@CoO yolk-shell nanostructures by injecting 1.08 g $Co_2(CO)_8$ in 6 ml of o-dichlorobenzene into the platinum nanocrystals solution, and followed by the oxidation of the product particles by blowing a stream of O_2/Ar mixture (1:4 in volume ratio, 120 ml/min) into the colloidal solution at 455 K. The system was kept at the same temperature under stirring for 3 hours.

Monocrystalline spinel nanotube fabrication
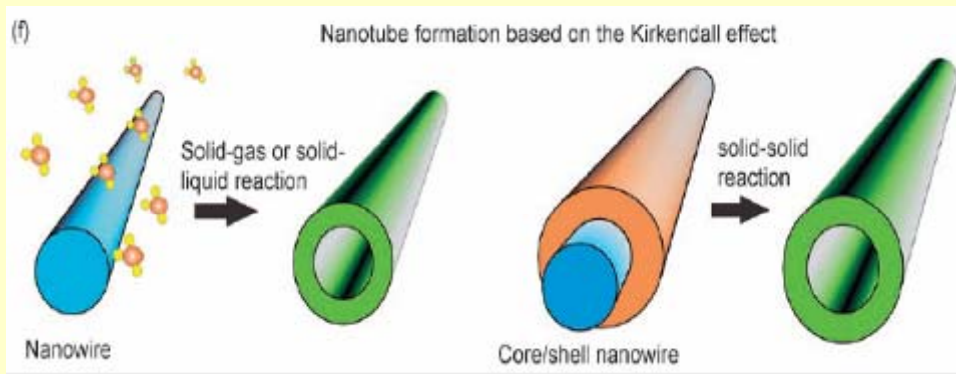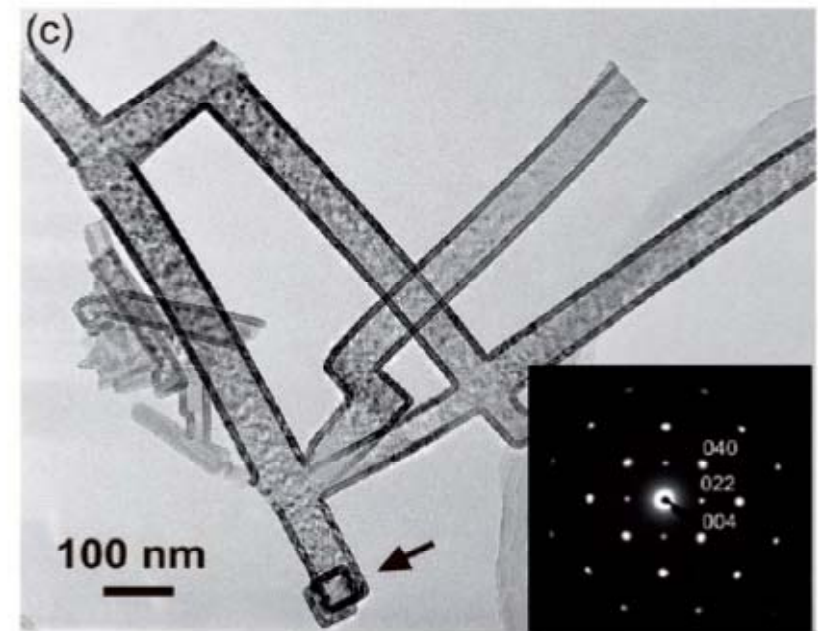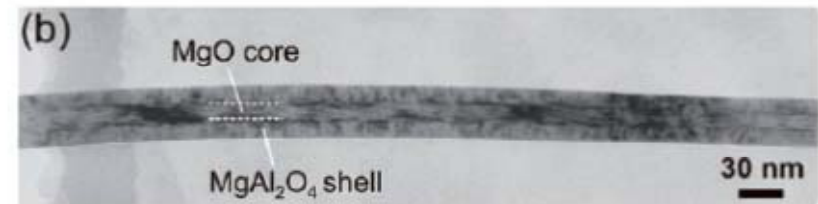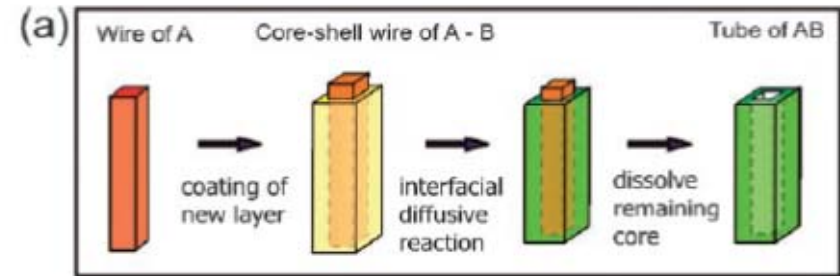# based on the Kirkendall effect. H.J. Fan, Nat. Mater. 5 (2006) 627-631
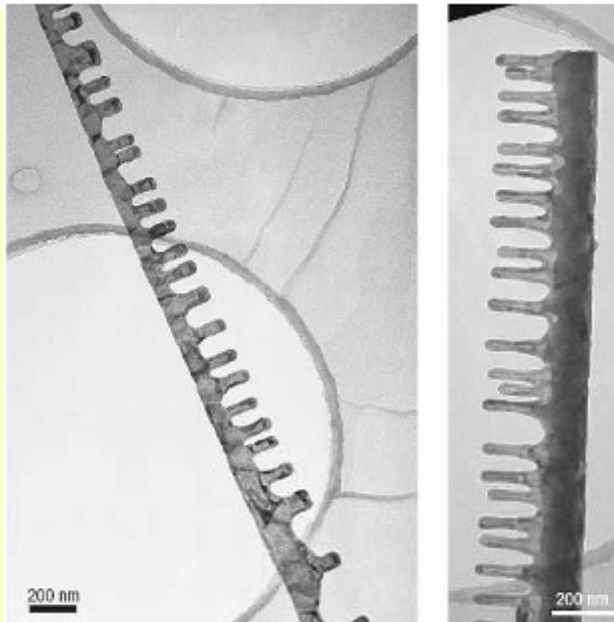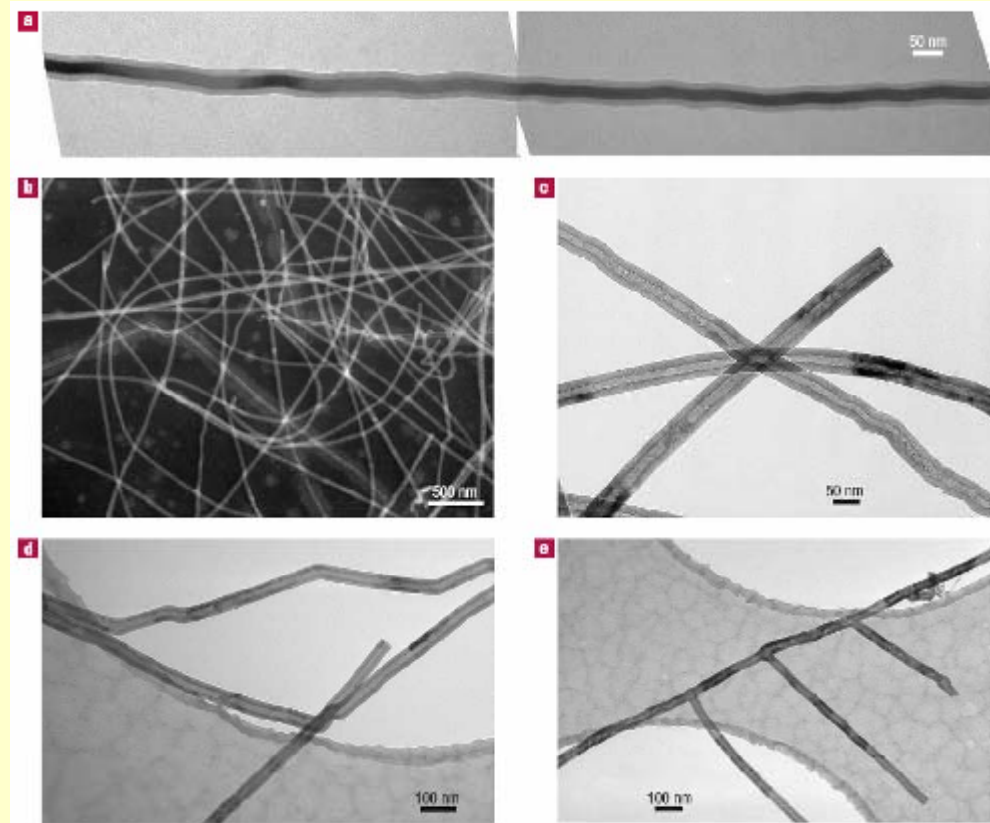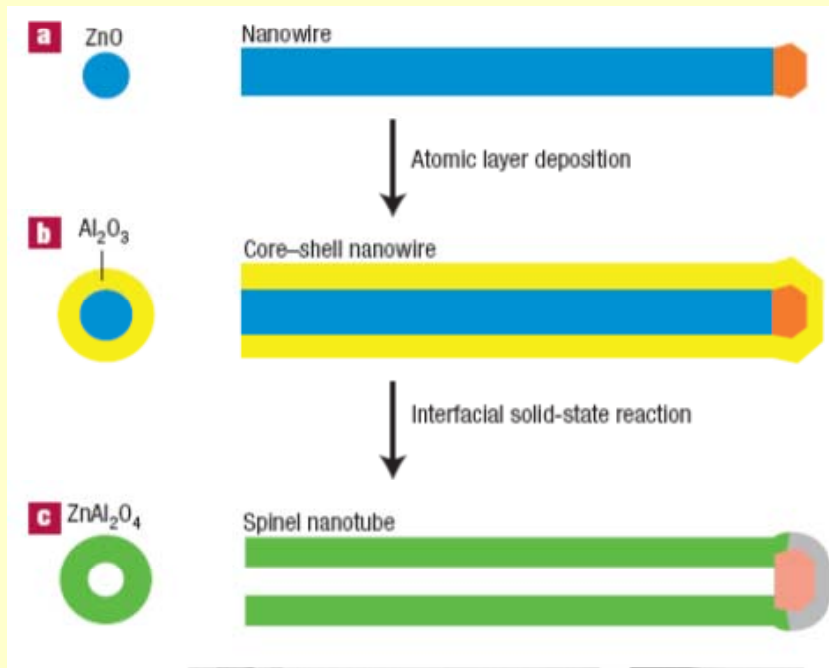
T_{annl} = 700 °C

T_m (Al_2O_3) = 2050°C

T_m (ZnO) = 1975°C (sublimation: 1800°C)

Formation of Nanotubes and Hollow Nanoparticles Based on Kirkendall and Diffusion Processes: A Review. H.J. Fan, Small 3 (2007) 1660-1671
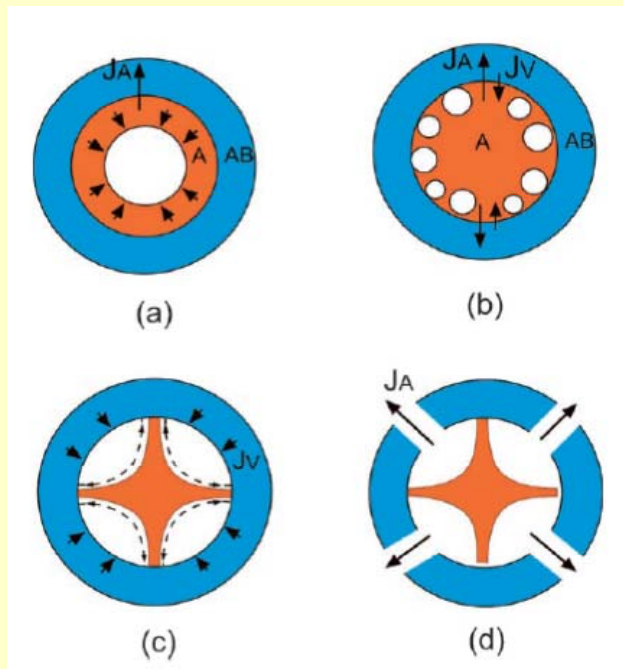
Based on Kirkendall effect

Based on Wagner cation counterdiffusion